Surface Science 184 (1987) 57–74
North-Holland, Amsterdam

THE MOLECULAR ADSORPTION OF NITROGEN DIOXIDE ON Pt(111) STUDIED BY TEMPERATURE PROGRAMMED DESORPTION AND VIBRATIONAL SPECTROSCOPY

M.E. BARTRAM, R.G. WINDHAM and B.E. KOEL

Cooperative Institute for Research in Environmental Sciences, and Department of Chemistry and Biochemistry, University of Colorado, Campus Box 449, Boulder, CO 80309-0449, USA

Received 15 September 1986; accepted for publication 15 December 1986

The adsorption of nitrogen dioxide (NO_2) on Pt(111) has been investigated using temperature programmed desorption (TPD) and high resolution electron energy loss spectroscopy (HREELS). At 100 K, NO_2 is adsorbed molecularly at all coverages to form a Pt(111) μ-N,O-nitrito surface complex. This puts NO_2 in an upright bridge-bonded configuration with C_s symmetry. Our assignment of this surface species is supported by the infrared spectrum of a μ-N,O-nitrito-platinate complex. The saturation coverage of chemisorbed NO_2 is about 0.5 monolayers (ML) at 100 K. At low coverages, $\theta_{NO_2} < 0.25$ ML, adsorption is irreversible and NO_2 dissociates completely by 285 K to O atoms and NO. However, at coverages greater than $\theta_{NO_2} = 0.25$ ML, the adsorption is partially reversible and NO_2 desorbs molecularly with first-order kinetics with $E_a = 19$ kcal/mol. About 20% of the NO_2 adsorbs reversibly at saturation coverage. With higher exposures of NO_2, a condensed multilayer of N_2O_4 can be formed.

1. Introduction

Only a few investigations have been made previously of the adsorption of nitrogen dioxide (NO_2) on transition metal surfaces [1–7]. This is somewhat surprising, since NO_2 is an extremely versatile ligand in inorganic chemistry, bonding to metal atoms in many distinct geometries [8]. Also, the chemistry that takes place between nitrogen oxides and noble metal surfaces impacts a number of technologically important areas. For instance, the three-way catalyst used to control automobile exhaust emissions uses the catalytic activity of Pt, Pd, and Rh in part to minimize the release of NO_x (NO, NO_2, N_2O_4) into the atmosphere [7,9,10]. In a more recent development, atmospheric scientists are now using gold catalysts to selectively reduce NO_y (NO_x and RNO_2 when R is a radical group) to NO using CO in order to make exceptionally sensitive atmospheric measurements [11]. A selective detector has also been developed recently [12,13] which makes use of selective oxidation of organic compounds by NO_2 in the presence of gold or palladium catalysts. Lack of molecular-level information on the interaction of NO_2 with metal surfaces has inhibited the

understanding of the mechanisms of catalytic reactions involving nitrogen oxides. This paper reports initial work of a comprehensive study of the surface chemistry of nitrogen oxides on the noble metals Pt, Pd, Rh, and Au.

In the most detailed work available, Schwalke et al. [3] used high resolution electron energy loss spectroscopy (HREELS) to study NO_2 adsorbed on Ru(001). The vibrational spectra obtained indicate that adsorption at 80 K is dissociative. At coverages near saturation, NO_2 dissociation ceases and NO_2 is adsorbed molecularly with C_{2v} symmetry through the nitrogen atom. A multilayer of N_2O_4 is formed at 80 K with increased exposure.

Two studies of NO_2 on Pt(111) have been performed previously. Segner et al. [1], using ultraviolet photoelectron spectroscopy (UPS), reported that NO_2 adsorption at 120 K was completely dissociative. Dahlgren and Hemminger [2] later used temperature programmed desorption (TPD) and low energy electron diffraction (LEED) to conclude that NO_2 adsorbed molecularly at 120 K but was completely dissociated by 240 K. In their studies, the desorption of molecular NO_2 was not observed at any coverage.

This paper presents TPD and HREELS data which presents a clearer picture of the adsorption and bonding of NO_2 on Pt(111). We unambiguously determine that NO_2 adsorbs molecularly at 100 K, and furthermore identify the adsorption geometry. This is the first observation of NO_2 being bridge-bonded to a metal surface upright with C_s symmetry. We support and greatly extend the previous work of Dahlgren and Hemminger [2]. However, in contrast to their results, we do observe about 20% of a monolayer of NO_2 to desorb reversibly near saturation coverage. We also put forward a possible explanation of the apparent contradiction produced by the previous UPS results of Segner et al. [1]. In a forthcoming paper, we will show how the Pt(111) surface can be modified to place NO_2 into a C_{2v} bonding geometry [14].

2. Experimental

The stainless steel UHV chamber is pumped by a 220 ℓs^{-1} ion pump and a titanium sublimation pump. The base pressure is typically 2×10^{-10} Torr. The two-level chamber is equipped with a 127° cylindrical sector spectrometer for HREELS, a double-pass cylindrical mirror analyzer (CMA) with an on-axis electron gun for Auger electron spectroscopy (AES), LEED optics, and a quadrupole mass spectrometer (QMS) with thoriated-iridium filaments for TPD. The crystal is heated resistively and is cooled by direct contact between the crystal holder and a liquid nitrogen reservoir. The crystal temperature is monitored by a chromel–alumel thermocouple. An IBM XT computer is used to perform TPD in a multiple-ion monitoring mode, to read the thermocouple, and to acquire Auger spectra.

The Pt(111) crystal was cleaned and annealed by a standard procedure [15]. After heating the crystal to 1000 K a number of times, no impurities were found to have diffused to the surface as determined by AES. Impurities that are difficult to detect by AES [16] were carefully looked for. The lack of an oxygen signal after heating in oxygen also helped to confirm the absence of elements such as Si, Ca, Al and Fe that form refractory oxides. Scanning high energy Auger transitions up to 2100 eV allowed the discrimination between Pt and elements such as S and P.

High purity NO_2 was synthesized [17] in a glass gas handling line that had been baked to a base pressure of 20 mTorr. O_2 (Scientific Gas Products, extra dry grade 99.6%) trapped in methanol–dry ice was mixed in a flow with NO (Scientific Gas Products, CP grade 99.0%) that was purified by passing it through silica gel trapped in methanol–dry ice. The reaction was run with an O_2 pressure twice that of the NO pressure to give a total reaction pressure slightly above ambient. This maintained a flow of excess O_2 out of the gas handling line. Crude NO_2 was collected in a trap immersed in methanol–dry ice as white N_2O_4 crystals contaminated with blue crystals of the $N_2O_3 \cdot NO$ adduct. The crude N_2O_4 was purified by passing trapped O_2 over it as it warmed up. The NO_2 was trapped again as pure white N_2O_4 crystals with methanol–dry ice. The NO_2 was stored in a stainless steel bottle that was first passivated with hot concentrated HNO_3. The stainless steel gas manifold on the UHV system was passivated in the same manner and then baked out prior to charging it with NO_2. The mass spectrometer intensity ratio of 4 for masses 30/46 was in close agreement with others [4,18] and established that the NO_2 was of a high purity.

The Pt(111) surface was exposed to NO_2 by means of a microcapillary array gas doser. This was done to minimize NO_2 decomposition by the chamber walls, filaments and the ion pumps. All of the exposures were done at 100 K. NO_2 exposures reported in langmuirs ($1\ L = 3.0 \times 10^{14}$ molecules/cm^2 for NO_2 at 298 K) were calculated in the following manner.

We first measured the surface oxygen coverage, θ_O, produced by a given exposure of NO_2 from the doser (measured by the uncorrected ion gauge). Then, assuming a sticking coefficient (S) of unity [1], the langmuirs of NO_2 required to give the measured θ_O were calculated. This calculation also provides an effective doser enhancement factor. Imbedded in it is the ion gauge sensitivity to NO_2 and the fraction of molecules which directly strike the crystal upon effusion from the doser. The unusually large doser enhancement [19] of 415 can be partly attributed to the high pumping speed of the chamber walls for NO_2. This also shows the necessity for using a microcapillary array doser.

Absolute surface coverages of adsorbates are ultimately referenced to values of θ_O. Calibration of θ_O was done by careful comparison to the TPD and XPS work of Gland [20] on the O_2/Pt(111) system, where $\theta_O = 0.25$ ML at

saturation coverage after desorption of the molecular oxygen state formed at 100 K. Using this calibration point for our own O_2/Pt(111) TPD data, the coverage of O atoms in our NO_2 work was measured from the relative areas of integrated O_2 TPD curves. Determination of θ_{NO_2} is made by fitting the data of fig. 3 to $S = 1$ independent of NO_2 coverage, and is further described in section 3.

TPD experiments were performed in line-of-sight of the QMS, approximately 4 cm away from the ionizer. The heating rates were 10 to 15 K/s. Masses 12, 14, 18, 28, 30, 32, 44 and 46 were monitored. No signals above background effects due to NO and NO_2 were detected from any masses except 14, 30, 32 and 46. Line-of-sight desorption into the ion gauge was also performed to show that all gases desorbing from the crystal were accounted for.

The HREELS spectra were recorded with a resolution of 80 cm^{-1}, a beam energy of 6 eV, and a beam current of 0.1 nA. The elastic peak typically had 10^5 counts for the clean Pt(111) surface. All of the spectra, including those of the warm-up experiments, were taken with the crystal at 100 K.

3. Results

3.1. Temperature programmed desorption

Fig. 1 shows the TPD spectra that were produced as a function of NO_2 exposure at 100 K. Initial adsorption of NO_2 is irreversible and no NO_2 desorption is observed at exposures lower than 1.5 L. Larger exposures lead to reversible adsorption of NO_2. Its desorption occurs with first-order kinetics and a desorption peak temperature of 320 K. Because the pumping speed for NO_2 is high (10 times that of NO), it was not possible to vary the heating rate significantly enough to determine the pre-exponential factor. Assuming it to be 10^{13} s^{-1}, the energy of activation for desorption would be 19 kcal/mol using Redhead analysis [21]. At a coverage near saturation of this state, desorption from a low temperature desorption state of NO_2 begins with an onset at about 125 K. Desorption from this state is shown more clearly in the top panel of fig. 1 and follows zero-order kinetics indicative of the formation of multilayers of NO_2. At exposures higher than 2.9 L, a third desorption state for NO_2 begins with an onset at 150 K. Qualitatively, it bears some resemblance to the NO_2 desorption seen by Schwalke et al. [3] except that in their case, this state is populated before the multilayer formed. We were not successful in attempts to desorb the multilayer without disturbing this state in order to investigate it with HREELS.

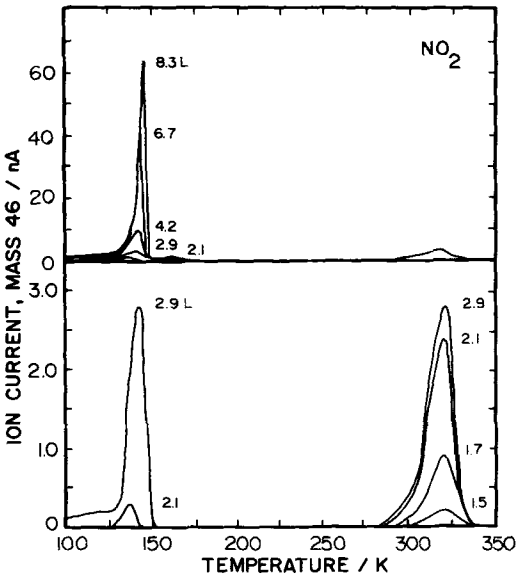

Fig. 1. NO_2 desorption spectra from Pt(111) for several NO_2 exposures at 100 K. The top panel shows clearly the zero-order desorption of NO_2 from a $N_2O_{4(s)}$ multilayer that takes place with an onset of 125 K for exposures larger than 2 L. The bottom panel shows the first-order desorption of NO_2 from the chemisorbed monolayer with a peak at 320 K.

The activation energy for NO_2 desorption of 19 kcal/mol obtained at high coverages is measured on essentially a passivated Pt(111) surface. This implies that the desorption energy on the clean Pt(111) surface could be higher than this. As it is, this energy is on the order of that predicted [1].

Fig. 2 shows TPD spectra of NO and O_2 that are produced from dissociation of NO_2. The amount of NO and O_2 formed increases with NO_2 exposure until 2.9 L. NO initially desorbs in a single state, β_2, which shifts from a temperature of 400 K to 320 K as the surface coverage increases. This peak shift indicates a decrease in the desorption energy for a first-order process, rather than simply being the result of second-order kinetics, since there is a dramatic shift of the high temperature tails of the desorption peaks. At higher coverages we see a new state, β_1, with a constant desorption peak temperature of 320 K. The small desorption peak in the NO desorption at 140 K in fig. 2 is due to the QMS cracking the NO_2 that desorbs from the multilayer. The activation energy for desorption of NO from NO_2 decomposition changes with coverage from 34 to 25 kcal/mol assuming that the pre-exponential factor 10^{16} s^{-1}, found for NO desorption from an NO exposure [22], is the same in this case.

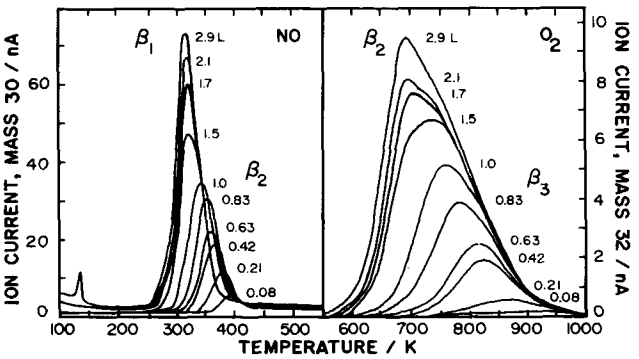

Fig. 2. NO and O_2 desorption spectra from Pt(111) for several NO_2 exposures at 100 K. The spectra were recorded simultaneously with those of fig. 1. The small NO peak at 140 K is due to a NO_2 cracking fraction from the desorption of the N_2O_4 multilayer.

O_2 desorbs initially in the β_3 state with second-order kinetics. However, after NO_2 exposures larger than 1.5 L, a high oxygen coverage β_2 state forms which has pseudo-first-order kinetics. The activation energy for O_2 desorption decreases from 51 to 41 kcal/mol in the β_3 state and is 39 kcal/mol for the β_2 state in agreement with previous results [15].

Fig. 3 summarizes the adsorbate coverages calculated from the TPD data shown in figs. 1 and 2 up to exposures of 5 L. The peak areas of the O_2

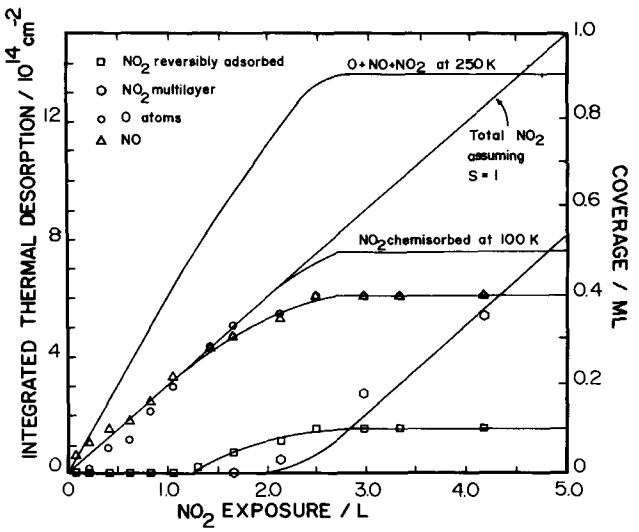

Fig. 3. Surface species concentrations on Pt(111) as a function of NO_2 exposure. The values are calculated by integration of the desorption spectra in figs. 1 and 2 and as described in the text.

desorptions were calibrated to give absolute surface coverages based on the XPS and TPD data on O_2/Pt(111) of Gland [20], as outline in section 2. The NO peak areas were normalized to the O_2 areas at saturation ($\theta_{NO} = \theta_O$), since no species, other than NO_2, was observed to desorb. The curve that results from these two sets of data represents the amount of NO_2 that dissociates on the surface during TPD. At saturation, this is 6.0×10^{14} NO_2 molecules/cm^2. Desorption of NO, O_2, and NO_2 remains constant for exposures of 2.5 L and higher. If one assumes that this is the exposure required to form the chemisorbed monolayer, and that the sticking coefficient is unity throughout this coverage region, an upper limit of 7.5×10^{14} molecules/cm^2 can be placed on the saturation coverage of NO_2 at 100 K. This scales the number of NO_2 molecules that desorb molecularly to an upper bound of 1.5×10^{14} NO_2 molecules/cm^2, or 20% of the saturation monolayer coverage.

Considering that the surface atom density for Pt(111) is 1.5×10^{15} atoms/cm^2, $\theta_{NO_2} = 0.5$ ML for a saturation dose of NO_2 at 100 K. Also plotted in fig. 3 is the sum of all surface species present in the monolayer at the onset of NO desorption (O atoms, NO, and NO_2). Until an initial coverage of $\theta_{NO_2} = 0.25$ ML is reached, decomposition of NO_2 to O atoms and NO proceeds without competition from any other process. It is at this point, where the total surface coverage is 0.5 ML, that molecular desorption of NO_2 begins to occur. Up to the onset of NO_2 and NO desorption, the coverage of total surface species may go as high as $\theta_{total} = 0.9$ ML. Also shown in fig. 3 is the population of NO_2 in the multilayer resulting from exposures up to 5 L. The straight line in fig. 3 was obtained using data up to the 8.3 L exposure. Fig. 3 also shows that some NO_2 desorption from $N_2O_{4(s)}$ occurs prior to complete saturation of the chemisorbed monolayer, indicating that dimerization begins to compete with chemisorption near saturation coverages in the monolayer.

3.2. *High resolution electron energy loss spectroscopy*

Fig. 4 presents a series of HREELS spectra as a function of NO_2 exposure at 100 K. The assignment of molecular adsorption is straightforward since there are no loss peaks due to NO. These would be present at 1490 and/or 1740 cm^{-1} (according to our NO/Pt(111) HREELS spectra and ref. [23]) if any decomposition had occurred. The peak at 485 cm^{-1} in the 0.18 L spectrum is due to the Pt–CO stretch from a trace amount of coadsorbed CO. The accompanying mode at 2100 cm^{-1} is not shown. Up to an exposure of 2.1 L, four loss peaks comprise each spectrum. In off-specular scans, all of these peaks were greatly attenuated and no other modes due to impact scattering were observed. Thus, all of the observed losses are due to dipole scattering. Molecularly adsorbed NO_2, bonded to the surface with C_s symmetry is the only structure that is consistent with this fact. In this bonding geometry, all of

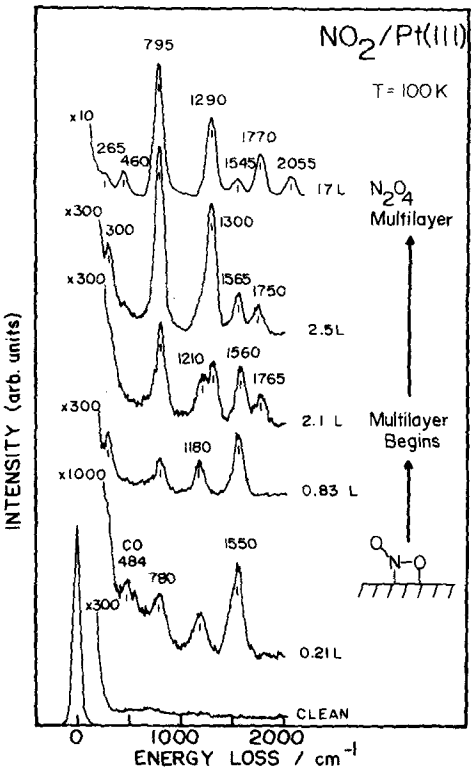

Fig. 4. HREELS spectra for increasing NO_2 exposures to Pt(111) at 100 K.

the modes of the surface complex are totally symmetric and are therefore observable in accordance with the surface dipole selection rule [24,25]. The frequency assignments are listed in table 1 with 300, 795, 1180, and 1560 cm^{-1} corresponding respectively to the Pt–N stretch, the ONO bend, the ONO symmetric stretch, and the ONO asymmetric stretch. The ONO bend at 795 cm^{-1} is 45 cm^{-1} higher than gas-phase NO_2, yet it is lower in frequency than that commonly found in transition metal complexes [8]. The frequency of the ONO bend has been observed to range from 817 to 863 cm^{-1} in these complexes with little dependence on the bonding geometry of NO_2. The large 380 cm^{-1} difference between the ONO symmetric and asymmetric stretches is classically associated with NO_2 that is strongly bound in a geometry of low symmetry [8].

Between the 0.21 and 0.83 L spectra, only small shifts in the frequencies occur. The relative intensities of the loss peaks also remain the same, while the absolute intensities increase by almost a factor of three, indicating that no large changes occur in the bonding of NO_2 as the coverage is increased.

At an exposure of 2.1 L, the intensity of the asymmetric ONO stretch relative to the other modes is lower than that seen in the spectra of NO_2 at lower coverages, indicating some change in bonding geometry occurs. Also, features of the multilayer are first seen. These grow in with increasing exposure until the intensities of these losses dominate the spectrum. These losses are due to the vibrational modes and combination bands of $N_2O_{4(s)}$. In the 2.5 L spectrum, the asymmetric stretch of C_s NO_2 is still visible at 1565 cm^{-1}. The symmetric stretch also remains visible as a shoulder on the low frequency side of the ONO symmetric stretch of N_2O_4 at 1300 cm^{-1}. Thus, the chemisorbed monolayer retains its bonding integrity as the condensation of the multilayer proceeds. The thick layer of $N_2O_{4(s)}$ that can be achieved at 100 K is made evident by the large inelastic loss intensity. The nature and phase of $N_2O_{4(s)}$ grown in UHV conditions have already been thoroughly discussed by Schwalke et al. [3], and will not be discussed further here.

Two HREELS warm-up experiments were performed to explore the low ($\theta_{NO_2} < 0.25$ ML) and the high coverage regimes within the NO_2 monolayer. The 0.83 L exposure shown in fig. 5 is representative of those TPD spectra in the low coverage regime where no NO_2 desorbs molecularly and the peak

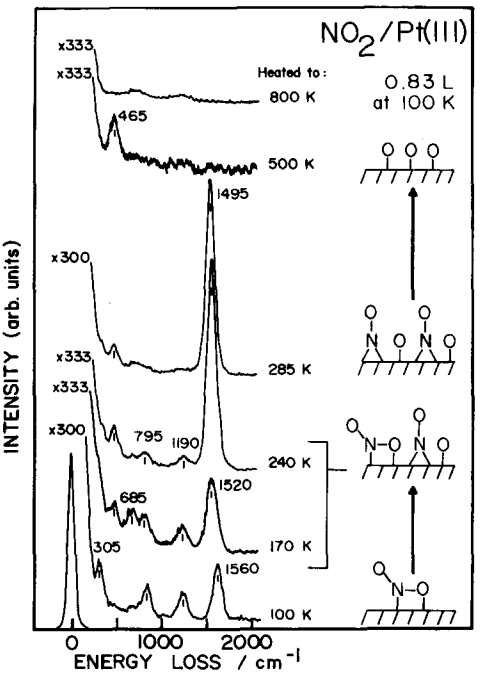

Fig. 5. HREELS warm-up experiments after 0.83 L NO_2 adsorbed on Pt(111) at 100 K. Dissociation begins by 170 K and by 285 K NO_2 is completely dissociated to O atoms and bridge-bonded NO.

temperature of desorption for NO shifts with prior NO_2 coverage. Consistent with fig. 4 for the same exposure at 100 K, the loss peaks can be assigned to C_s NO_2. Upon warming to 170 K, two new loss features at 465 cm^{-1} and at 685 cm^{-1} can be seen. A 40 cm^{-1} shift in the asymmetric stretching peak down to 1520 cm^{-1} can be seen as well. While we have no definitive assignment for the 685 cm^{-1} loss, it is clearly due to an ONO bending mode. The spectrum may be due to a rehybridized intermediate in the beginning of NO_2 decomposition to NO and O. The peak at 465 cm^{-1} is due to the Pt–O stretch. The 1520 cm^{-1} peak may also have some contribution from the growing 1495 cm^{-1} peak seen for the 240 K warm-up. By 240 K decomposition is significant as seen in the intense loss at 1495 cm^{-1} which is due to bridge-bonded NO. Losses due to C_s NO_2 are only minor features in the spectrum. At 285 K, all of the NO_2 has decomposed and losses from NO_2 can no longer be seen. At 500 K, all of the NO has desorbed and only the Pt–O stretch can be seen at 465 cm^{-1}.

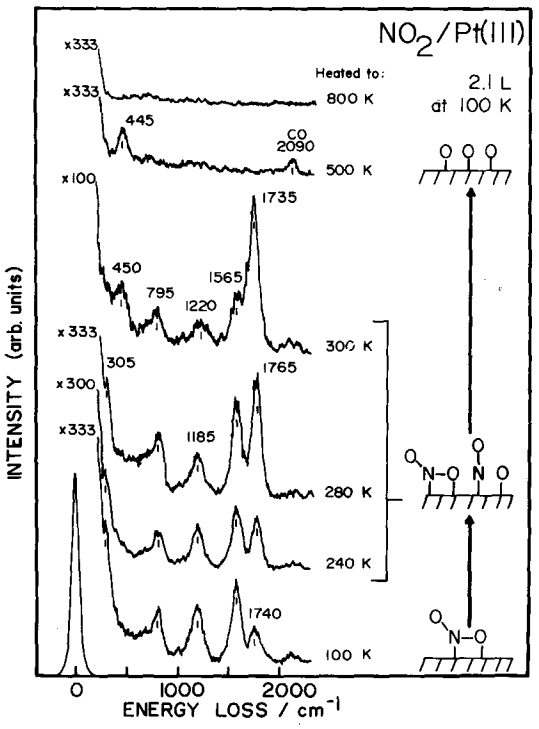

Fig. 6. HREELS warm-up experiments after 2.1 L NO_2 adsorbed on Pt(111) at 100 K. At this high coverage, some molecularly adsorbed NO_2 remains even at 300 K. NO from NO_2 dissociation occupies atop sites.

The HREELS warm-up that examines the high coverage case (2.1 L) where NO_2 both decomposes and desorbs molecularly is shown in fig. 6. This experiment begins with a near saturation coverage of NO_2 coadsorbed with some top-site bonded NO impurity seen at 1740 cm^{-1}. As made evident by an increase in intensity of the NO loss, decomposition begins by 240 K. As the surface temperature is raised, decomposition puts NO only in atop sites, without detection of bridge-bonded NO. The NO stretch shifts up 25 cm^{-1} as the surface becomes more crowded with the products of NO_2 decomposition at 240 K. By 300 K, when desorption of some NO and NO_2 has occurred (a change in the total surface coverage of about a third), the NO stretch shifts back down to 1735 cm^{-1}. A substantial amount of molecular C_s NO_2 is still present at 300 K, consistent with TPD conclusions. The frequency of the NO_2 symmetric stretch is shifted up by 35 cm^{-1} due to bonding changes induced by coadsorption with O and NO.

LEED studies were performed which are consistent with the HREELS and TPD data. For exposures near 1.5 L, a 2×2 LEED pattern begins to form at 240 K and becomes very sharp at 280 K. This is consistent with the previous LEED results of Dahlgren and Hemminger [2]. However, HREELS shows clearly that decomposition noticeably begins as low as 170 K for lower NO_2 coverages.

4. Discussion

4.1. Adsorption geometry of molecular NO_2 on Pt(111)

In transition metal coordination compounds, NO_2 coordinated in the form of NO_2^- (nitrite) is an extremely versatile ligand due to its ambidentate properties. Nitrite has the potential to coordinate to a metal in nine different ways [8]. With the exception of nitrite bridge-bonded through the oxygen atoms and three-coordinate nitrite located between two coordination centers, all of these possibilities have unambiguous examples of their structures.

Chemisorption of NO_2 on the Pt(111) surface should remove its radical character to the degree that it may be effectively treated as nitrite. Nitrite could be adsorbed in three different ways that would yield a geometry with the C_s symmetry that is necessary to achieve the number of dipole active modes detected with HREELS. These three isomers, μ-N,O-nitrito, nitrito, and three-coordinate nitrite are illustrated schematically in fig. 7. Although there are few examples [8,26], μ-N,O-nitrito is the most prevalent type of bridge formed by nitrite in transition metal coordination compounds. Coordinate-covalent bonds of sigma symmetry between N and the metal leave the N atom sp^2 hybridized and a double bond between the N atom and the non-coordinated O. The inequality of the N–O bonds that this creates comes out in the

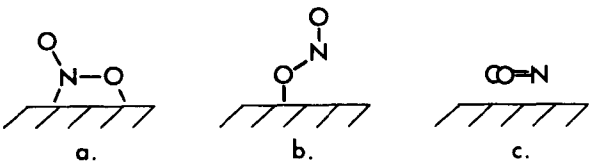

Fig. 7. Schematic models of the three possible NO_2 surface complexes which have C_s symmetry: (a) μ-N,O-nitrito, (b) nitrito, and (c) three-coordinate nitrite.

infrared spectra of these compounds as a 200 to 389 cm^{-1} difference between the symmetric and asymmetric stretching frequencies in the range of 1148 to 1537 cm^{-1}. This is in significant contrast to the 67 cm^{-1} difference that exists between these two modes of uncoordinated nitrite in $NaNO_2$. Nitrito coordination to a transition metal, as in fig. 7b, can split these modes by as much as 400 cm^{-1}. However, Pt complexes containing nitrito are known to be thermodynamically unstable, as are many other nitrito coordinated complexes. There is no example of three-coordinate nitrite bonded exclusively to metal centers. In the geometry indicated by fig. 7c, the perpendicular components of the dipole moments associated with the asymmetric and symmetric stretches would be small giving loss peaks of weak intensity. The equivalent N–O bonds would be expected to have a vibrational spectrum very much like non-bonded nitrite with its stretching modes within 100 cm^{-1} of each other in the region of 1300 cm^{-1}. There appears to be no reasonable bonding scheme for this adsorption geometry that would not be predicted to lead to decomposition or reorientation. In view of this perspective, the μ-N,O-nitrito isomer is the most consistent with the HREELS spectra we have obtained. In accordance with inorganic nomenclature [8,27] this specific adsorption geometry yields a Pt(111) μ-N,O-nitrito surface complex.

This assignment is supported by an excellent agreement between the HREELS data and the stretching frequencies of the bridging nitrito groups found in potassium tri-μ-nitro-μ_3-oxo-cyclo-tris[nitroplatinate(II)]trihydrate [28] given in table 1. The Pt–N stretch and the ONO bend were not assigned

Table 1
Comparison of the vibrational frequencies (cm^{-1}) of μ-N,O-nitrito surface species on Pt(111) with those of the bridge-bonded NO_2 cobalt [26] and platinum [28] complexes

Mode	Gas phase [30] NO_2	Coordination compounds		Pt(111) μ-N,O-nitrito
		$[Co(NH_3)_3(OH)_2NO_2]_2^{3+}$	$K_2[Pt_3(NO_2)_6O]$	
ν M–NO_2 (stretch)	–	500	–	300
δ NO_2 (bend)	750	830	–	795
ν_sONO (sym. stretch)	1318	1200	1148	1180
ν_aONO (asym. stretch)	1618	1516	1537	1560

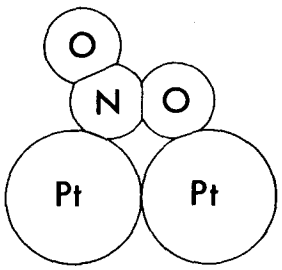

Fig. 8. Tentative model for the Pt(111) μ-N,O-nitrito surface complex, illustrated using covalent radii. Estimates of the bond angles and lengths relative to the Pt–Pt distance are based on those found in μ-N,O-nitrito transition metal coordination compounds [8,26].

for this salt. The frequencies of the ONO stretching modes are very close to those of a bridging nitrito cobalt complex [26]. The vibrational frequencies of this complex are also listed in table 1. The ONO bending mode of the cobalt complex at 830 cm^{-1} agrees nicely with our 795 cm^{-1} mode of adsorbed NO_2.

A tentative model for the Pt(111) μ-N,O-nitrito surface complex is shown in fig. 8 using covalent radii. The measured value of $\theta_{NO_2} = 0.5$ ML at saturation of the chemisorbed layer is consistent with the stoichiometry of the Pt(111) μ-N,O-nitrito surface complex, as shown in fig. 8. In addition, the coverage expected for a two-dimensional NO_2 liquid can be calculated by taking the 2/3 root of the liquid density to provide a value of 7.10×10^{14} molecules/cm^2, or $\theta_{NO_2} = 0.5$ ML. Fig. 8 demonstrates that NO_2 could be packed along the surface efficiently enough to achieve this coverage.

In lieu of single crystal X-ray diffraction data on the platinum salt, the bond angles and lengths relative to the Pt–Pt distance shown in fig. 8 are estimated from transition metal compounds that contain μ-N,O-nitrito groups [8,26]. C_s symmetry for the μ-N,O-nitrito species requires the molecular plane of NO_2 to be perpendicular to the surface. This should leave the N atom in a state of sp^2 hybridization with a double bond between the non-coordinated O atom and the N atom. Therefore, bonding of NO_2 to two Pt atoms on the surface is expected to be of the di-sigma type restricting the surface complex to a rigid conformation and a well defined binding site. The ONO bond angle for coordinated nitrite is influenced greatly by steric factors and is typically 115° or less [8]. The steric bulk of the surface might be expected to influence the ONO bond angle similarly, in which case the N=O component would only be 25° off normal. Obviously, the adsorption of NO_2 greatly destroys the equivalence of the 2 N–O bonds. The frequency difference between the two stretching modes of NO_2 in the surface complex bears this out, since an almost linear relationship is known to exist between the bond length differences and the corresponding stretching frequency differences in coordinated nitrite [8,29]. With the N=O approaching perpendicular and the lengthening of

the N–O bond that is parallel to the surface, the μ-N,O-nitrito species can be seen as a logical precursor to dissociation. Facile formation of this species may explain molecular beam studies of the steady-state decomposition of NO_2 on Pt(111) at higher temperatures which reveal that the rate limiting step for the process is the desorption of NO [1].

It may be anticipated that the molecular orbitals of NO_2 undergo a radical change upon adsorption and bear little resemblance to the molecular orbitals of NO_2 in the gas phase. In this case, UPS would understandably provide information similar to that expected for dissociated NO_2. This may explain the apparently contradictory conclusion of Segner et al. [1] that was mentioned in the introduction of this paper (section 1), if one discounts other possible artifacts in the UPS work such as radiation-induced dissociation or NO-contaminated NO_2. In view of this possibility, we are beginning a combined HREELS/UPS study which would be important to determine the nature of the extensive rehybridization of the molecular orbitals that occurs upon molecular NO_2 chemisorption on Pt(111).

4.2. Adsorption kinetics and intermolecular interactions at 100 K

The initial sticking coefficient of NO_2 is essentially unity (> 0.97) independent of temperature below 300 K. At 100 K, the sticking coefficient remains unity independent of coverage, as shown in fig. 3. A precursor state was attributed by Segner et al. [1] to be responsible for the high dissociative sticking coefficient for NO_2 observed on Pt(111) at 300 K and above, and would also explain our results. The linkage isomers of nitrite found in transition metal complexes present the possibility that numerous weakly bound analogs to these isomers may also exist for adsorbed NO_2. Although they are not stable on the HREELS time-scale, short-lived adsorption intermediates such as these may dominate the uptake kinetics. Thus, a large number of adsorption geometries that interact favorably with the surface may explain the origin of the high sticking coefficient for NO_2.

The observation of NO_2 desorption characteristic of the N_2O_4 multilayer before reaching complete saturation of the chemisorbed monolayer, implies that NO_2 dimerization may become competitive with NO_2 chemisorption as monolayer coverage is approached and the heat of adsorption is decreased. An activated process involving an initial formation of N_2O_4 to give NO_2 at a higher temperature can be ruled our since the HREELS spectra provide no evidence of N_2O_4 at low exposures. This does not remove the possibility that at coverages near saturation some rearrangements of the NO_2 monolayer may occur to allow additional NO_2 from the multilayer to occupy the monolayer upon warming. (As shown in the following, this would be thermodynamically favorable.) LEED observations show no indication of long range order at any coverages from 100 to 240 K. Loss features due to NO_2 in the monolayer that

can still be seen as the multilayer coverage increases, do not shift in frequency. This implies that the chemical bonding in the monolayer remains essentially unperturbed; chemisorbed NO_2 is not noticeably incorporated into the N_2O_4 multilayer. This is consistent with the thermodynamic relationship between NO_2 and N_2O_4. We have determined that the activation energy for NO_2 desorption is a minimum of 19 kcal/mol. Since the adsorption is essentially non-activated (less than 2 kcal/mol) the heat of adsorption is at least 19 kcal/mol. In the gas phase, NO_2 dimerization to form N_2O_4 liberates 14 kcal/mol. Therefore, the formation of N_2O_4 from an NO_2 molecule from the gas phase or from a weakly held precursor state and one from the surface would give a heat of reaction of +5 kcal/mol, while its formation from two NO_2 molecules from the surface would give a heat of reaction of +24 kcal/mol. This assumes, of course, that no interaction of the dimer with the surface occurs. The experimental observation that NO_2 dimerization does not begin until the surface is nearly saturated implies that this interaction would be weak, on the order of van der Waals interactions.

The preceding discussion further supports our assignment of a μ-N,O-nitrito surface complex. This orientation on the surface is the only C_s symmetry possibility that provides both a fixed conformation and a minimum of surface space occupancy. The adsorption of NO_2 with its molecular plane parallel to the surface as in fig. 7c would be sensitive enough to the surface coverage to produce noticeable changes in the HREELS spectra and allow it to dimerize easily. It would also fill more space on the surface than the proposed complex. The adsorption of NO_2 through only an O atom, as in fig. 7b, would leave the N center in the molecule open for reaction from several approaches to form the dimer. Free rotation about the Pt–O bond would allow it to occupy a large area at low coverages while, at high coverages, its conformational possibilities would become highly coverage dependent. This would be reflected in the HREELS spectra by changes in loss energies and intensities with coverage.

4.3. NO_2 decomposition pathways

Two distinct regimes are observed in the behavior of NO_2 on Pt(111). At low coverages, $\theta_{NO_2} < 0.25$ ML, irreversible NO_2 adsorption leads to coadsorbed NO and O upon heating during TPD. NO is bound in a bridge-site and its binding energy is very sensitive to the surface coverage of O. This leads to an 80 K shift in peak temperature for the β_2 state. When $\theta_{NO_2} > 0.25$ ML, formation of the β_2 O_2 desorption state begins. This signals a large O atom coverage from decomposition of larger amounts of NO_2 and two changes in the surface chemistry occur as a result. First, NO no longer occupies the β_2 state but instead desorbs in the β_1 state where it is bound in atop sites and is insensitive to increasing amounts of coadsorbed O. Importantly, NO_2 desorption becomes competitive with the dissociation channel, leading to some

reversible adsorption at high NO_2 coverages. The fact that saturation is reached at the same time for O_2, NO, and NO_2 says that there is no coverage where dissociation and molecular desorption cease being competitive. It is not clear whether the higher O atom coverage or the higher total O + NO coverage formed from initial dissociation decreases the ability of the Pt surface to decompose NO_2. However, oxygen atoms, since they are very strongly adsorbed, should dominate the modifying effects on the surface reactivity.

The NO desorption states that result from NO_2 dissociation are essentially the same as those seen when Pt(111) is exposed to NO [23]. The desorption maxima of the respective β_1 and β_2 states are similar and the β_2 state is occupied first as well. But, in contrast to NO_2/Pt(111), the desorption energy of the β_2 state is not significantly changed as more NO is adsorbed, nor is the β_1 state occupied to the exclusion of β_2. The sensitivity of NO to coadsorbed O observed in our study is similar to that reported by Gorte et al. [22] in their coadsorption study of CO and NO. They observed that the temperature for desorption of NO could be lowered by as much as 100 K in the presence of CO.

The O_2 desorption states are the same as the two high temperature O_2 desorption states that can be seen after exposing Pt(111) to NO_2 at 440 K [1,14]. This high temperature exposure can also produce a third state, β_1, to give a total saturation O atom coverage of 0.77 ML. The saturation O atom coverage achieved in our work is about half of this at 0.4 ML. To contrast this further, $\theta_O = 0.25$ ML at saturation from O_2 exposure at 100 K and $\theta_O = 0.5$ ML using extended temperature cycling at around 150 K or when external atomization is used [20].

4.4. Temperature dependence of NO_2 catalytic reactions

In these UHV experiments, we have observed large changes in the population of adsorbates produced by NO_2 exposure dependent on the surface temperature. Thus, elementary processes in catalytic reactions of NO_2 are expected to be modified greatly depending on the catalyst temperature. Of course, at higher pressures, these temperature regions would be markedly changed and the populations of surface species would also be greatly affected by the gas-phase concentrations.

We have observed three interesting temperature regimes in our UHV studies in which the concentration of potentially reactive surface species changes. At temperatures less than 240 K, molecular NO_2 is the dominant species. The lability of the O atom bound to the surface in the μ-N,O-nitrito surface complex, however, may make it amenable to selective oxidation reactions. This proposed lability is supported by Dahlgren and Hemminger [2], who have proposed an NO_2 intermediate to explain the desorption of $N^{18}O$ at 325 K from their $NO_2 + {}^{18}O_2$ coadsorption experiments. In the temperature

range of 240 to 400 K, the composition of the adsorbed layer varies significantly with temperature. Therefore, under some conditions, catalytic reactions of NO_2 may be extremely sensitive to temperature. At high temperatures, above 400 K, O atoms are the dominant species. As mentioned previously, O atom coverages up to $\theta_O = 0.77$ ML can be produced in UHV from NO_2 exposures at high temperatures. At these high coverages, oxygen is bound more weakly to the Pt surface and would be more labile for catalytic oxidation reactions than the O atoms present at low oxygen coverages. Thus, at least at high temperatures, O atoms may be important oxidizing species.

The influence of coadsorbed O atoms on surface reactions may also make the catalysis dependent on the thermal history of the catalyst. For example, we will show in a subsequent paper [14] that preadsorbed O atoms dramatically change the NO_2 and Pt(111) surface chemistry, forming a C_{2v} bonded NO_2 species that is reversibly adsorbed.

5. Summary

New information concerning NO_2 coverage, adsorption geometry and energetics, and dissociation pathways on Pt(111) has been obtained from this TPD and HREELS study. The important points of this work are:

- NO_2 is adsorbed molecularly on Pt(111) at 100 K in a bridge-bonded configuration through an O atom and the N atom with C_s symmetry in an upright position.
- θ_{NO_2} is 0.5 ML at saturation of the chemisorbed monolayer at 100 K. This agrees with the stoichiometry of the proposed Pt(111) μ-N,O-nitrito surface complex. A multilayer of $N_2O_{4(s)}$ can be formed at higher exposures.
- At low coverages ($\theta_{NO_2} < 0.25$ ML), NO_2 dissociates completely to bridge-bonded NO and O by 285 K.
- At high coverages ($\theta_{NO_2} > 0.25$ ML), NO_2 desorption becomes competitive with dissociation and has an activation energy of 19 kcal/mol. NO formed from NO_2 dissociation is bound at an atop site. A maximum of 20% of the NO_2 in the chemisorbed monolayer desorbs reversibly at a saturation coverage.

Acknowledgements

The authors wish to thank Fred Fehsenfeld for useful discussions and Carleton J. Howard and the members of his research group for their help and advice in synthesizing NO_2. Acknowledgement of Jeff Kingsley, Jay Lindquist, and John Hemminger for software to perform multiple-ion monitoring TPD

and AES is given with appreciation. Partial financial support for this work by the National Acid Precipitation Assessment Program and Sievers Research, Inc. is gratefully acknowledged.

References

[1] J. Segner, W. Vielhaber and G. Ertl, Israel J. Chem. 22 (1982) 375.
[2] D. Dahlgren and J.C. Hemminger, Surface Sci. 123 (1982) L739.
[3] U. Schwalke, J.E. Parmeter and W.H. Weinberg, J. Chem. Phys. 84 (1986) 4036.
[4] U. Schwalke, H. Niehus and G. Comsa, Surface Sci. 152/153 (1985) 596.
[5] U. Schwalke, N. Niehus and G. Comsa, in: Desorption Induced by Electronic Transitions, Eds. W. Brenig and D. Menzel (Springer, Berlin, 1985) p. 98.
[6] J.C. Fuggle and D. Menzel, Surface Sci. 79 (1979) 1.
[7] C.R. Brundle and A.F. Carley, Faraday Disc. 60 (1975) 51.
[8] M.A. Hitchman and G.L. Rowbottom, Coordination Chem. Rev. 42 (1982) 55.
[9] W.F. Egelhoff, Jr., in: The Chemical Physics of Solid Surfaces and Heterogeneous Catalysis, Eds. D.A. King and D.P. Woodruff (Elsevier, Amsterdam, 1982) p. 397.
[10] K.C. Taylor, in: Catalysis: Science and Technology, Vol. 5, Eds. J.R. Anderson and M. Boudart (Springer, Berlin, 1984) p. 120.
[11] M.J. Bollinger, R.E. Sievers, D.W. Fahey and F.C. Fehsenfeld, Anal. Chem. 55 (1983) 1980.
[12] S.A. Nyarady and R.E. Sievers, J. Am. Chem. Soc. 107 (1985) 3726.
[13] R.E. Sievers, S.A. Nyarady, R.L. Shearer, J.J. DeAngeles and R.M. Barkley, J. Chromatogr. 349 (1985) 395.
[14] M.E. Bartram, R.G. Windham and B.E. Koel, to be published.
[15] C.T. Campbell, G. Ertl, H. Kuipers and J. Segner, Surface Sci. 107 (1981) 220.
[16] M. Mundschau and R. Vanselow, Surface Sci. 157 (1985) 87.
[17] C.J. Howard, personal communication.
[18] A. Cornu and R. Massot, Compilation of Mass Spectral Data (Heyden, London, 1979).
[19] C.T. Campbell and S.M. Valone, J. Vacuum Sci. Technol. A3 (1985) 408.
[20] J.L. Gland, Surface Sci. 93 (1980) 487.
[21] P.A. Redhead, Vacuum 12 (1962) 203.
[22] R.J. Gorte, L.D. Schmidt and J.L. Gland, Surface Sci. 109 (1981) 367.
[23] J.L. Gland and B.A. Sexton, Surface Sci. 94 (1980) 355.
[24] H. Ibach and D.L. Mills, Electron Energy Loss Spectroscopy and Surface Vibrations (Academic Press, New York, 1982).
[25] B.E. Koel, in: Scanning Electron Microscopy/1985/IV (SEM, AMF O'Hare, IL, 1985) p. 1421.
[26] K. Nakamoto, J. Fujita and H. Murata, J. Am. Chem. Soc. 80 (1958) 4817.
[27] N.R. Avery, J. Vacuum Sci. Technol. A3 (1985) 1459.
[28] A.E. Underhill and D.M. Watkins, J. Chem. Soc., Dalton Trans. (1977) 5.
[29] A.J. Finney, M.A. Hitchman, C.L. Raston, G.L. Rowbottom and A.H. White, Australian J. Chem. 34 (1981) 2125.
[30] E.T. Arakawa and A.H. Nielsen, J. Mol. Spectrosc. 2 (1958) 413.